THERMOFORMING SIMULATION OF THERMOPLASTIC TEXTILE COMPOSITES

P. Boisse[1*], P. Wang[1, 2], N. Hamila[1],

[1] *Laboratoire de Mécanique des Contacts et des Solides, INSA-Lyon, F-69621, France*
[2] *University of Lille, ENSAIT, GEMTEX, F-59056, France*
* *E-mail address: Philippe.Boisse@insa-lyon.fr*

Keywords: Thermoplastic; Prepreg; Thermoforming; Finite element analysis;

Abstract
Thermoforming CFRTP prepreg is a fast manufacturing process compared to LCM process or thermoset prepreg forming. The duration of the thermoplastic forming process can be in the range of one minute. In addition the composites with thermoplastic matrix are more easily recyclable than thermoset materials. A simulation approach for thermoforming of multilayer thermoplastic is presented. Each prepreg layer is modeled by semi-discrete shell elements. A lubricated friction model is implemented between the layers and for ply/tool friction. Thermal and forming simulations are presented and compared to experimental results. The computed shear angles after forming and wrinkles are in good agreement with the thermoforming experiment. It will be shown by the comparison of two simulations that the temperature field play an important role in the process quality..

1 Introduction

The forming processes of composite materials by stamping thin structures are complex operations involving many parameters. Geometries of the tools and of the blank-holder, loading on the tools, as well as the lubrication (and many other parameters) must be optimized in order to guarantee the success of the process. In the case of composites with continuous fibers and thermoplastic matrix (CFRTP), other parameters such as the temperature, the applied pressure as well as the stacking sequence are supplementary parameters that have a main importance in the process result quality. The development of a numerical simulation software in order to determine the feasibility of a given geometry associated to a set of satisfactory parameters proves to be essential in order to reduce the development costs of a new process. This numerical simulation software will also allow the knowledge of the state of material in the final part. Since thirty years, the finite element method appears to be an effective framework for the simulation of the forming processes and in particular sheet metal forming [1]. In the case of the composites a numerical simulation software for the forming simulation of the thin parts will have to be able to predict the final orientation of fibers that will determine the mechanical properties of the final part. It will also have to predict wrinkling, the final thickness and the final quality of the product (presence of porosities, possible rupture of fibers). The manufacturing process of a thermoplastic composite is made at hot temperature and requires a stage of heating followed by a punch and die stamping operation. Then a phase of reconsolidation of the stack of plies consists in a transverse compression of the composite.

The present paper presents an approach for the thermoforming of thermoplastic prepregs [2]. For the single ply deformation, it is based on the methods that have been developed for the simulations of the forming of dry textile reinforcements in LCM processes [3, 4]. This approach was extended to the forming simulations of multilayer continuous fibre reinforcements with thermoplastic resin composites taking into account thermal and viscous effects and contact/friction between the plies. Forming simulations need a description of the mechanical behaviour of the composite ply during forming. As this ply is generally modeled by shell finite elements, the mechanical behaviour of the prepreg ply during forming is given by biaxial tensile properties [5,6], in-plane shear properties [7-9] and bending properties [10]. The bending stiffness is low because of the possible motions between the fibers, but it is important in the determination of the size of wrinkles [11]. In-plane shear is the most important deformation mode to obtain double curved shapes. In thermoplastic prepreg forming simulations, the in-plane shear properties of the ply must be measured at high temperatures because the forming is performed above the melt temperature of the matrix.

2. Semi-discrete shell finite elements

This approach takes into account the difficulties to describe the textile material as a continuum in one hand (continuous approach) and the difficulties to model all the yarns and their contacts in the other hand (discrete approach). In this approach that is more or less intermediate, the textile composite reinforcement is seen as a set of a discrete number of unit woven cells submitted to membrane loadings (i.e. biaxial tension and in-plane shear) and bending (Fig. 1) [3].

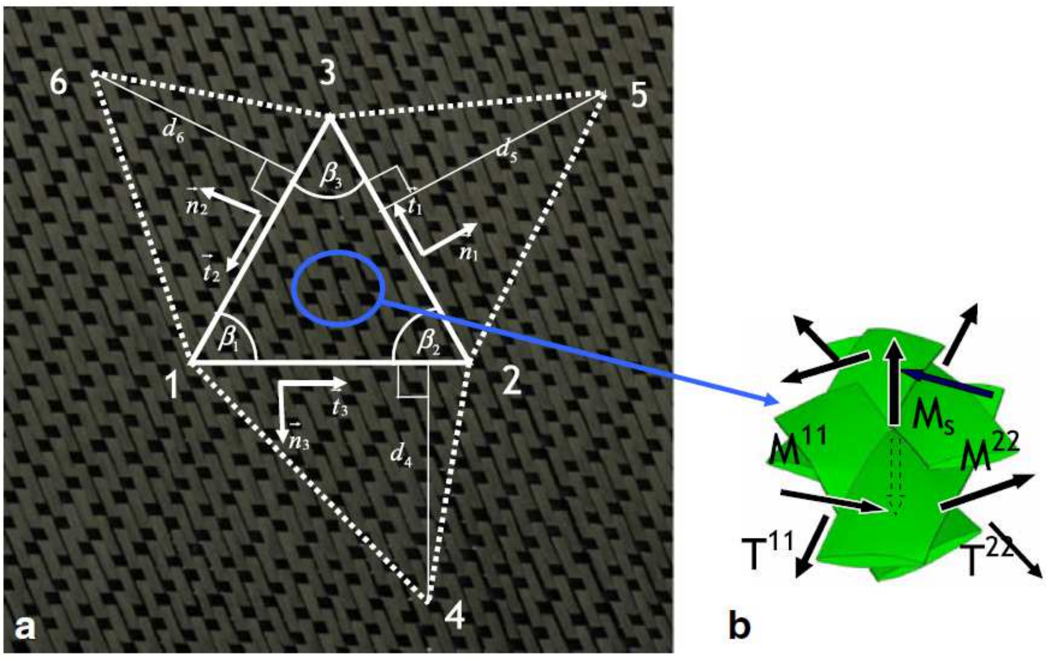

Figure 1. Semi-discrete triangular element

In any virtual displacement field $\underline{\eta}$ such as $\underline{\eta}$ = 0, the internal virtual work is assumed in the form:

$$W_{int}(\underline{\eta}) = W_{int}^{t}(\underline{\eta}) + W_{int}^{s}(\underline{\eta}) + W_{int}^{b}(\underline{\eta}) \quad (1)$$

$W_{int}^{t}(\underline{\eta})$, $W_{int}^{s}(\underline{\eta})$, $W_{int}^{b}(\underline{\eta})$ are the internal virtual works of biaxial tension, in-plane shear and bending respectively. For a reinforcement or prepreg made of ncell woven cells:

$$W_{int}^{t}\left(\underline{\eta}\right) = \sum_{p=1}^{ncell} {}^{p}\varepsilon_{11}\left(\underline{\eta}\right) {}^{p}T^{11}\,{}^{p}L_1 + {}^{p}\varepsilon_{22}\left(\underline{\eta}\right) {}^{p}T^{22}\,{}^{p}L_2 \quad (2)$$

$$W_{int}^{s}\left(\underline{\eta}\right) = \sum_{p=1}^{ncell} {}^{p}\gamma\left(\underline{\eta}\right) {}^{p}M^{s} \quad (3)$$

$$W_{int}^{t}\left(\underline{\eta}\right) = \sum_{p=1}^{ncell} {}^{p}\chi_{11}\left(\underline{\eta}\right) {}^{p}M^{11}\,{}^{p}L_1 + {}^{p}\chi_{22}\left(\underline{\eta}\right) {}^{p}M^{22}\,{}^{p}L_2 \quad (4)$$

$\varepsilon_{11}(\underline{\eta})$ and $\varepsilon_{22}(\underline{\eta})$ are the virtual axial strains in the warp and weft directions. $\gamma(\underline{\eta})$ is the virtual angle between warp and weft directions. $\chi_{11}(\underline{\eta})$ and $\chi_{22}(\underline{\eta})$ are the virtual curvatures of warp and weft yarns. L_1 and L_2 are the length of unit woven cell in warp and weft directions. Experimental tests specific to textile composite reinforcements are used to obtain these mechanical properties. Biaxial tensile tests give the tensions T^{11} and T^{22} in function of the axial strain ε_{11} and ε_{22}, the picture frame or the bias extension test gives the shear moment M^{s} in function of the angle change γ between warp and weft yarns and the bending tests give the bending moments $M^{11}$and M^{22} in function respectively of χ_{11} and χ_{22}.
The three node triangle shown Fig.1. is composed of ncelle woven cells. The virtual generalized strains $\varepsilon_{11}(\underline{\eta})$, $\varepsilon_{22}(\underline{\eta})$, $\gamma(\underline{\eta})$, $\chi_{11}(\underline{\eta})$ and $\chi_{22}(\underline{\eta})$ can be related to the virtual nodal displacements of the nodes of the element taking into account the interpolation of the geometric and kinematic conditions within the element.

3. Contact and viscous friction modeling

The numerical modeling of contact/friction behaviour during the forming process is accomplished using the forward increment Lagrange multipliers algorithm proposed by Carpenter *et al.* [12]. This approach is introduced into the dynamic equation as contact occurs.

$$\begin{aligned} &[M]\{\ddot{u}_n\} + \{F_n^{int}\} + [G_{n+1}]^T\{\lambda_n\} = \{F_n^{ext}\} \\ &[G_{n+1}](\{u_{n+1}\} + \{X_0\}) = \{0\} \end{aligned} \quad (5)$$

where $\{u\}$ is the vector of displacement degrees of freedom, $\{X_0\}$ is the initial co-ordinate vector of the nodes, [M] is the mass matrix, $\{F^{int}\}$ and $\{F^{ext}\}$ are internal and external loads vectors, $\{\lambda\}$ is the vector of Lagrange multipliers. Its components are slave nodal contact forces, n is the index of the time step, [G] is a surface contact displacement constraint matrix.

In the case of "semi-implicit" integration, the total displacement of each node is calculated by a predictor $\{u^*\}$ determined from Eq. (5) and a corrector $\{u^c\}$.

$$\begin{aligned}
&\{u_{n+1}\} = \{u^*_{n+1}\} + \{u^c_{n+1}\} \\
&\{u^*_{n+1}\} = \Delta t^2 [M]^{-1}(\{F^{ext}_n\} - \{F^{int}_n\}) + 2\{u_n\} - \{u_{n-1}\} \\
&\{u^c_{n+1}\} = -\Delta t^2 [M]^{-1}[G_{n+1}]^T \{\lambda_n\}
\end{aligned} \tag{6}$$

where Δt is a time step increment. Eqs. (5) and (6), lead to a linear solution of contact forces (Eq. (7)). Subsequently, the calculations of contact forces and the corrector of the total displacement are performed using the Gauss-Seidel iteration algorithm.

$$\Delta t^2 [G_{n+1}][M]^{-1}[G_{n+1}]^T \{\lambda_n\} = [G_{n+1}](\{u^*_{n+1}\} + \{X_0\}) \tag{7}$$

$$\left\{\Delta\lambda^{i \to i+1}\right\} = \left\{F^T_C\right\} + F^N_C \left\{n\right\} - \left\{\lambda^i\right\} \tag{8}$$

where F^N_C is the normal contact force, $\{n\}$ is the normal direction of contact surface and $\{F^T_C\}$ is the tangential contact force vector on the slave node.

Using the variation of contact forces between iterations i and i+1 ($\Delta\lambda^{i \to i+1}$), the total displacement at increment n+1 can be obtained by Eq. (9):

$$\begin{aligned}
&\left\{\Delta u^c\right\} = -\Delta t^2 [M]^{-1}[G_{n+1}]^T \left\{\Delta\lambda^{i \to i+1}\right\} \\
&\left\{u^c\right\}_{i \to i+1} = \left\{u^c\right\}_i + \left\{\Delta u^c\right\}_{i \to i+1} \\
&\left\{u_{n+1}\right\} = \left\{u^*_{n+1}\right\} + \left\{u^c_{n+1}\right\}
\end{aligned} \tag{9}$$

Taking into account the viscous friction between (tool / ply) and (ply / ply) interfaces is very important in the numerical modelling of thermoplastic composite forming. Some experiments have shown that the thermoplastic composite forming is in the hydrodynamic lubrication range described on the generalised Stribeck curve [13, 14]. Thus a lubricated friction model is implemented between two solid surfaces. In this case, the effective friction coefficient on tool / ply and ply / ply interfaces can be described by

$$\begin{aligned}
&\mu_{eff} = C_1 H_e + C_2 \\
&H_e = \frac{\eta V}{F_N}
\end{aligned} \tag{10}$$

where H_e is the Hersey number, which depends on the resin viscosity η, the velocity between two contact surfaces V and the normal load applied F_N. C_1 and C_2 are two constants determined by a pull-out experiment.

The relative velocity between the two contact surfaces is known from the total displacement of the slave node contacting with a master surface. The vector of tangential contact force $\{F^T_C\}$ on a pair of slave / master surface can be modelled as:

$$\left\{F^T_C\right\} = -(C_1 \cdot \eta \cdot \left\|\overline{V}\right\| + C_2 \cdot F^N_C) \cdot \frac{\overline{V}}{\left\|\overline{V}\right\|} \tag{11}$$

where $\overline{V}$ is the relative velocity. The viscosity of the matrix is assumed to be linear in function of the temperature in the temperature range of the process.

4. Thermoforming simulation

The following thermoforming simulations are performed on 5-harness satin / PEEK (polyetheretherketone) prepregs. The in-plane shear behaviour at different temperatures for 5-harness satin/PEEK prepregs has been characterized by bias-extension tests [9].

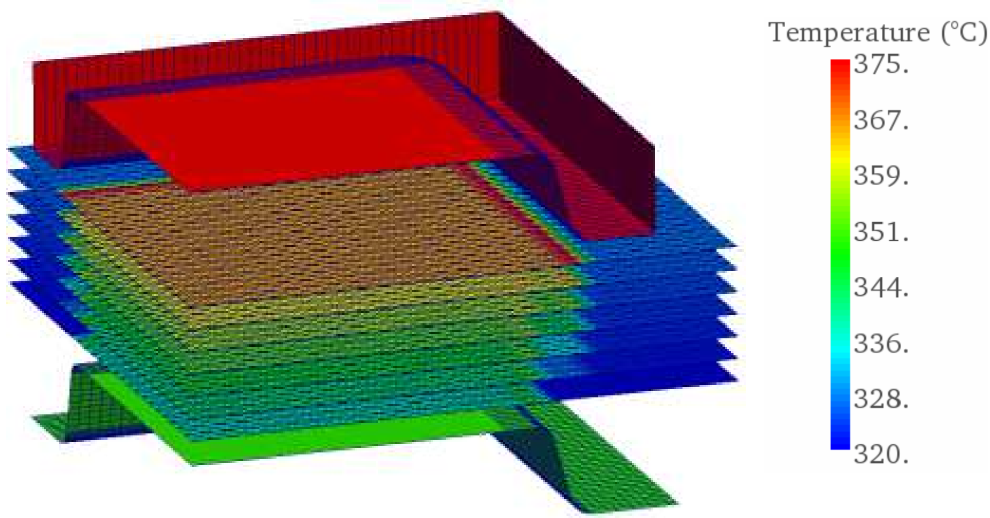

Figure 2. Temperature distribution in each ply at the beginning of the forming stage.

The geometry of the tools is shown in Fig. 2. This forming is performed for 7 carbon/PEEK prepreg plies by a punch with a bowl shape. The preheating simulation of the prepreg stack is performed taking into account conduction and convection effects. Fig. 2 presents the temperature distribution in the prepreg stack obtained by numerical simulation. This temperature is not uniform (between 320 and 375 °C). The computed values are in good agreement with the experiment [2]. A temperature gradient is present through the thickness of the prepreg stack and between the central region and the edges of ply. This is in good correlation with the experimental measurements. The local temperature at each point of the prepreg will be taken into account in the forming simulation.
The agreement between the final shape of the composite part obtained by numerical simulation with the experiments is good. Furthermore, a correct correlation is obtained for the maximum shear angle between the numerical simulation (48°) and experiments (42°) (Fig. 3). Wrinkling is one of the most common flaws that occur during textile composite forming processes [11]. The numerical and experimental analyses of wrinkling during this industrial thermoforming benchmark are presented in Fig. 4.

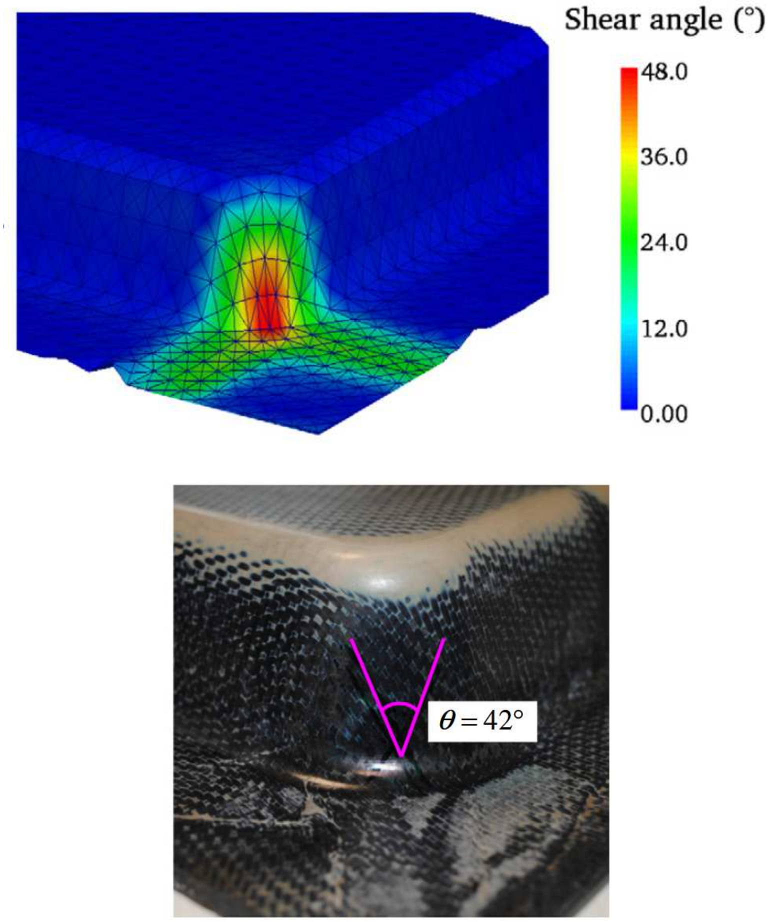

Figure 3. Comparison of the maximum shear angle

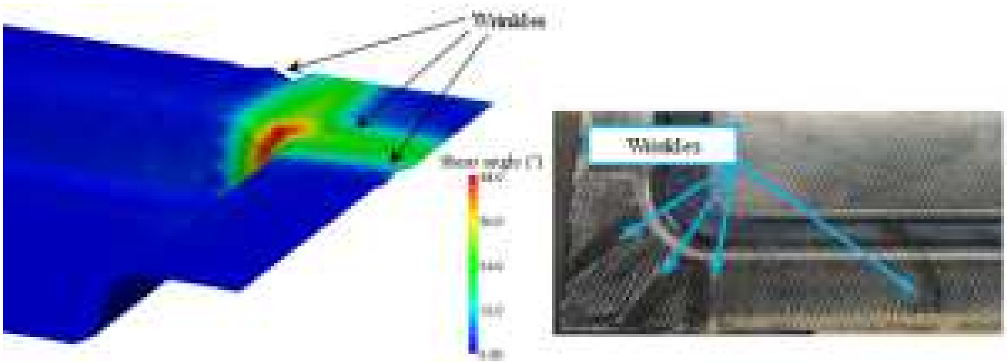

Figure 4. Numerical / experiment comparison of wrinkling phenomena at the end of forming.

Wrinkles can be observed in both numerical and experimental analyses at the beginning of the forming process as well as in the final composite part. The correlation between the numerical simulation and experiments concerning the wrinkles is correct. Numerical simulations can highlight the wrinkle onsets and developments during a thermoforming process and consequently permit to optimize the process parameters to avoid these defects at least in the useful zone. Some more details on the simulation and comparison with thermoforming process can be found in [2].

Conclusion

It is important to predict the feasibility conditions of the prepreg composite forming through numerical simulation analysis. The numerical simulation can improve the understanding of the forming process. On the other hand it gives some essential forming information, such as temperature, final shape of the laminate, direction of the fibres at all points of the different layers and possible wrinkling phenomena. The forming simulations have pointed out the significant importance of thermal conditions during the forming process. The temperature field must be taken into account in a very accurate manner in this simulation. In the presented approach, it is assumed that the forming process is fast enough to consider the temperature field constant in a given point during forming. Ideally the thermal and mechanical analyses should be fully coupled.

Acknowledgements

The research work reported in this paper was partly supported in the scope of the project CRISTAL (FUI)

References

[1] Wagoner R, Chenot J L, Fundamentals of metal forming analysis, 1996, Wiley.
[2] P Wang, N Hamila, P Boisse, Thermoforming simulation of multilayer composites with continuous fibres and thermoplastic matrix, Composites Part B, 2013, 52, 127–136.
[3] Hamila N, Boisse P, Sabourin F, Brunet M. A semi-discrete shell finite element for textile composite reinforcement forming simulation. Int J Numer Methods Eng 2009;79:1443–66.
[4] S Allaoui, P Boisse, S Chatel, N Hamila, G Hivet, D Soulat, E Vidal-Salle, Experimental and numerical analyses of textile reinforcement forming of a tetrahedral shape, Composites Part A, 2011, 42, 612-622
[5] Carvelli V, Corazza C, Poggi C. Mechanical modelling of monofilament technical textiles. Comput Mater Sci 2008;42:679-91.
[6] Willems A, Lomov SV, Verpoest I, Vandepitte D. Optical strain fields in shear and tensile testing of textile reinforcements. Compos Sci Technol 2008;68:807-19.
[7] Lomov SV, Willems A, Verpoest I, Zhu Y, Barburski M, Stoilova Tz. Picture frame test of woven composite reinforcements with a full-field strain registration. Text Res J 2006; 76 (3):243-52.
[8] Cao J, Akkerman R, Boisse P, Chen J, et al.. Characterization of Mechanical Behavior of Woven Fabrics: Experimental Methods and Benchmark Results. Compos Part A 2008; 39:1037-53.
[9] Wang P, Hamila N, Pineau P, Boisse P. Thermo-mechanical analysis of thermoplastic composite prepregs using bias-extension test. J Thermo Compos Mate, DOI: 10.1177/0892705712454289, 2012.
[10] de Bilbao E, Soulat D, Hivet G, Gasser A. Experimental Study of Bending Behaviour of Reinforcements. Exp Mech 2010;50:333-51.
[11] Boisse P, Hamila N, Vidal-Sallé E, Dumont F. Simulation of wrinkling during textile composite reinforcement forming. Influence of tensile, in-plane shear and bending stiffnesses. Compos Sci Technol 2011;71(5):683-92.
[12] Carpenter N. J, Taylor R. L, Katona M. G. Lagrange constraints for transient finite element surface contact. Inter J Numer Methods Eng 1991; 32:103-28.
[13] Gorczyca-Cole JL, Sherwood JA, Chen J. A friction model for thermostamping commingled glass-polypropylene woven fabrics. Compos Part A 2007;38:393-406.
[14] ten Thije RHW, Akkerman R, Van der Meer L, Ubbink MP. Tool-ply friction in thermoplastic composite forming. Int J Mater Form 2008; Suppl 1: 953-56